Austrian Journal of Statistics
2026, Volume 55, Issue 3, 65–90.
http://www.ajs.or.at/

A Novel Multivariate Generalized Circular Mixed Model for Count Data: Classical & Bayesian Inferences

Subhrajit Saha
Department of Statistics,
Visva Bharati
Santiniketan, India

Debashis Chatterjee
Department of Statistics,
Visva Bharati
Santiniketan, India
S. N. Bose National Centre for Basic Sciences,
Kolkata, 700106, WB, India

Abstract

This paper introduces a novel multivariate generalized circular mixed model (GCMCM) framework for analyzing count data with underlying directional components. The proposed methodology addresses gaps in traditional count models that overlook angular dependencies by integrating circular distributions with count-based observations. We develop a generalized mixed-model framework, integrating multivariate circular data and count responses through logical and rigorous Bayesian inference. The model is particularly applicable in fields such as ecology and neuroscience. The theoretical properties, estimation techniques, and applications are discussed in detail, highlighting computational challenges and advancements.

Keywords: multivariate circular data, count data, mixed models, Bayesian inference, directional statistics, von Mises distribution, Poisson regression, random effects, Python, R.

1. Introduction

Count-based responses with inherent directional components are prevalent across disciplines such as ecology, neuroscience, and environmental science. While standard Poisson and negative binomial regressions are robust for linear predictors, they fail to account for the periodic nature of directional data, such as animal movement angles or neuronal firing orientations. Neglecting these circular dependencies typically leads to biased parameter estimates and a failure to capture the true underlying spatial or temporal topology of the system.

Despite the development of independent models for count and circular data, few integrated frameworks exist to jointly handle multivariate directional-count dependencies. This research addresses this gap by proposing the Multivariate Generalized Circular Mixed Model (GCMCM). The GCMCM incorporates a circular structure into a generalized linear mixed model (GLMM) framework, allowing for the simultaneous modeling of multiple directional predictors and count responses that may exhibit overdispersion or subject-level correlation.

The proposed framework utilizes a hierarchical Bayesian approach to account for between-subject variability via random effects, which is critical for longitudinal or repeated measures data common in biological studies. Furthermore, the GCMCM is designed to resolve the unique identifiability challenges inherent in circular data, such as multimodal posterior surfaces and periodicity. By providing a mathematically grounded approach to multivariate circular-count inference, this model offers a robust alternative to traditional linearization methods.

The novelty and contributions of this work are fourfold:

1. **Integrated Topology:** Development of the GCMCM framework to explicitly handle the non-linear interplay between multivariate directional predictors and Poisson-distributed responses.

2. **Bayesian Identifiability:** Implementation of a robust Bayesian inferential scheme using weakly informative von Mises priors to resolve the non-identifiability issues inherent in circular location parameters.

3. **Hierarchical Flexibility:** Integration of subject-specific random effects to capture within-subject variability, extending circular models to longitudinal and repeated-measures designs.

4. **Computational Efficiency:** Implementation of efficient MCMC sampling techniques that overcome the computational bottlenecks typically associated with high-dimensional circular-linear likelihoods.

By addressing these challenges, the GCMCM provides a statistically rigorous foundation for analyzing complex phenomena where directionality and frequency are intrinsically linked.

2. Related works

The statistical analysis of data integrating count responses with directional predictors sits at the intersection of Generalized Linear Mixed Models (GLMMs) and directional statistics. While both fields have matured independently, their synthesis remains a burgeoning area of research.

2.1. Advances in circular and linear mixed modeling

The extension of GLMMs to handle complex data structures has been widely explored in classical frequentist frameworks. da Silva, Laureano, Petterle, Ribeiro Jr, and Bonat (2023) and Antonio and Beirlant (2007) demonstrated the versatility of GLMMs in modeling multivariate count data and longitudinal actuarial structures, respectively, by using random effects to capture inherent correlations. In the context of spatial data, dimensionality reduction of random effects has been a primary focus to mitigate spatial confounding and computational intensity Hughes and Haran (2013); Guan and Haran (2018).

In directional statistics, modeling circular responses often involves wrapped or projected distributions. Sikaroudi and Park (2021) utilized wrapped normal distributions for linear-circular regression, while Maruotti (2016) and Picone (2013) extended these concepts to longitudinal and incomplete multivariate marine data using projected normal mixtures. Despite these advances, these models primarily focus on circular outcomes rather than circular predictors influencing a discrete count response. Regression models based on the multivariate von Mises distribution (Lagona 2016) have addressed correlated circular data but often lack the hierarchical depth required for multi-subject count observations.

2.2. Bayesian approaches to circular-count data

Bayesian inference offers a robust alternative for hierarchical modeling, particularly when dealing with the non-linearities of circular parameters. Recent developments have focused on high-dimensional and compositional count data, often addressing zero-inflation in microbiome or omics studies (Silverman 2019; Koslovsky 2023; Li, Jiang, Koh, Xiao, and Zhan 2019). Robustness in these models is frequently achieved through the use of Dirichlet process priors (Antonelli, Trippa, and Haneuse 2016) or reparameterized geometric distributions to handle outliers (Oppen 2020).

In the circular domain, Bayesian clustering for non-ordered multivariate data has been successfully implemented using hierarchical projected normal distributions (Abraham, Servien, and Molinari 2019). Furthermore, the use of probabilistic programming languages like Stan has facilitated the customization of complex psychometric and functional mixed models (Jiang, Ouyang, Shi, Shi, Zhang, Xu, and Cai 2024; Lee, Miranda, Rausch, Baladandayuthapani, Fazio, Downs, and Morris 2019). However, a significant gap remains: existing Bayesian frameworks rarely provide a unified approach for multivariate circular predictors within a mixed-effects count model. Our proposed GCMCM

fills this void by integrating von Mises prior structures with a hierarchical Poisson-link framework, specifically designed to resolve the identifiability issues inherent in angular components.

3. Multivariate circular foundations

To capture the dependencies between multiple angular predictors within the GCMCM, we utilize the Multivariate von Mises (MvM) distribution. This distribution serves as the directional analogue to the multivariate Gaussian, providing a mathematically rigorous periodic framework for high-dimensional angular data. Simulations and applications use independent von Mises circular covariates for computational tractability; the multivariate von Mises formulation is included as the natural extension when circular predictors exhibit cross-dependence.

3.1. The multivariate von Mises (MvM) distribution

We adopt the Eight-Parameter (or Cosine) model variant (Mardia, Hughes, Taylor, and Singh 2008) for a p-dimensional random vector of angles $\boldsymbol{\theta} = (\theta_1, \ldots, \theta_p)'$. The joint density function is defined as:

$$f(\boldsymbol{\theta}|\boldsymbol{\mu}, \boldsymbol{\kappa}, \mathbf{K}) \propto \exp\left(\sum_{i=1}^{p} \kappa_i \cos(\theta_i - \mu_i) + \sum_{i<j} K_{ij} \cos(\theta_i - \theta_j - (\mu_i - \mu_j))\right),$$

where $\boldsymbol{\mu} \in [0, 2\pi)^p$ denotes the vector of mean directions and $\boldsymbol{\kappa} \in \mathbb{R}^p_{>0}$ represents the concentration parameters. The interaction matrix $\mathbf{K} = [K_{ij}]$ serves as the directional analogue to the precision matrix in Gaussian distributions, capturing the pairwise dependencies between angular variables and allowing the model to account for correlated directional inputs (Lagona 2016).

3.2. Computational inference and challenges

Inference in MvM models is historically constrained by the intractability of the normalizing constant, which involves complex integrals of modified Bessel functions. While maximum likelihood estimation (MLE) is feasible for low dimensions, it becomes computationally prohibitive as the dimensionality p increases.

Following Navarro, Frellsen, and Turner (2017), we utilize a Bayesian framework to circumvent these limitations. By employing Markov Chain Monte Carlo (MCMC) methods, we obtain posterior distributions for the concentration and interaction parameters. This approach is essential for our GCMCM framework, as it allows for the integration of weakly informative priors to ensure identifiability in the presence of high-dimensional count responses—a critical requirement for complex applications in ecology and bioinformatics (Mardia *et al.* 2008; Lagona 2016).

4. Bayesian inference and prior selection

To estimate the parameters of the GCMCM, we adopt a hierarchical Bayesian approach. This framework is particularly advantageous for handling the latent random effects and the periodic constraints of the circular predictors. We specify prior distributions to incorporate structural constraints while ensuring model identifiability.

4.1. Prior specifications and identifiability

For the regression coefficients and the covariance structures associated with the random effects and circular dependencies, we assume the following conjugate and weakly informative priors:

$$\boldsymbol{\beta} \sim N(\mathbf{0}, \sigma^2\mathbf{I}), \quad \mathbf{D} \sim \text{Inverse-Wishart}(v_0, \mathbf{S}_0), \quad \boldsymbol{\Lambda} \sim \text{Wishart}(\nu_0, \mathbf{S}_0).$$

A critical methodological challenge in circular-linear models is the non-identifiability of the location parameter under circular uniform priors, which lack a unique resultant mean direction. To resolve this, we implement a weakly informative von Mises prior for the circular mean parameters $\boldsymbol{\mu}$:

$$\mu_k \sim vM(\mu_0, \kappa_0), \quad k = 1, \ldots, p,$$

where κ_0 is set to a diffuse value (e.g., 0.1). This choice provides a mathematically well-defined location parameter while remaining non-prescriptive, allowing the data to dominate the posterior estimation of the mean direction.

The joint posterior distribution is proportional to the likelihood function and the product of the independent priors:

$$p(\boldsymbol{\beta}, \mathbf{D}, \boldsymbol{\mu}, \boldsymbol{\Lambda} | \mathbf{Y}, \mathbf{Z}, \mathbf{X}) \propto \mathcal{L}(\boldsymbol{\Theta} | \mathcal{D}) \cdot p(\boldsymbol{\beta}) \cdot p(\mathbf{D}) \cdot p(\boldsymbol{\mu}) \cdot p(\boldsymbol{\Lambda}).$$

4.2. Computational implementation

Posterior estimation was conducted via Markov Chain Monte Carlo (MCMC) sampling using the `JAGS` (Just Another Gibbs Sampler) engine interfaced through `R`. To ensure structural stability and global convergence across the multimodal posterior surfaces characteristic of directional data, we initialized three parallel chains with over-dispersed starting values.

Each chain was run for $20,000$ iterations, with the first $5,000$ discarded as burn-in. Convergence was monitored through visual inspection of trace plots and the Gelman-Rubin diagnostic ($\hat{R} < 1.05$). Data synthesis and circular descriptive analytics were facilitated by the `circular` and `Rfast` computational libraries.

5. Model diagnostics and goodness-of-fit

The structural integrity of the GCMCM is evaluated through a multi-tiered diagnostic framework. Given the complexity of multivariate circular-linear dependencies, we utilize

predictive checks and information criteria to assess the adequacy of the hierarchical Poisson-link structure.

5.1. Posterior predictive distribution and residuals

We evaluate the generative performance of the model using the posterior predictive distribution, defined as $p(\tilde{\mathbf{Z}}|\mathbf{Y},\mathbf{Z},\mathbf{X}) = \int p(\tilde{\mathbf{Z}}|\theta)p(\theta|\mathbf{Y},\mathbf{Z},\mathbf{X})\,d\theta$. Posterior predictive checks (PPC) are employed to compare replicated count data $\tilde{Z}$ with observed values Z. To assess the variance-mean relationship and identify influential observations, we compute Pearson residuals:

$$r_{ij} = \frac{Z_{ij} - \mathbb{E}[Z_{ij}]}{\sqrt{\mathrm{Var}(Z_{ij})}}.$$

A random distribution of residuals around the zero line confirms that the subject-specific random effects b_i and the weakly informative von Mises priors successfully capture the data's heterogeneity.

5.2. Information criteria: DIC and WAIC

To facilitate model selection and complexity penalization, we report the Deviance Information Criterion (DIC) (Spiegelhalter, Best, Carlin, and Van Der Linde 2002) and the Watanabe-Akaike Information Criterion (WAIC) (Watanabe and Opper 2010). While DIC remains a standard for Bayesian mixed models, WAIC is particularly advantageous for the GCMCM as it utilizes the full posterior distribution, providing a more robust measure for high-dimensional circular dependencies.

As noted in our results, the convergence of these metrics serves as an indicator of posterior stability and appropriate penalization of the subject-specific random effects, ensuring that the inclusion of multivariate angular predictors does not lead to overfitting.

5.3. Overdispersion and the negative binomial extension

To account for instances where the variance exceeds the mean—a common phenomenon in environmental and biological count data—we extend the Poisson link to a Negative Binomial (NB) structure:

$$\mathrm{Var}(Z_{ij}) = \lambda_{ij} + \frac{\lambda_{ij}^2}{\phi},$$

where ϕ is the dispersion parameter. As $\phi^{-1} \to 0$, the model recovers the Poisson structure. This flexibility allows the GCMCM to accommodate the extra-Poisson variability inherent in directional-count datasets without compromising the recovery of the circular mean directions $\boldsymbol{\mu}$.

6. Simulation 1

The simulation focuses on Bayesian inference for count data with circular predictors.

6.1. Data generating process

To evaluate the performance of the proposed GCMCM framework for count data with circular predictors, we simulated a dataset consisting of $n = 100$ subjects and $p = 3$ circular variables. The circular variables, denoted as $\mathbf{Y}_i = (Y_{i1}, Y_{i2}, Y_{i3})'$, are modeled as being drawn from the von Mises distribution. The probability density function is:

$$f(Y_{ik} \mid \mu_k, \kappa_k) = \frac{1}{2\pi I_0(\kappa_k)} \exp\left(\kappa_k \cos(Y_{ik} - \mu_k)\right),$$

where $I_0(\cdot)$ is the modified Bessel function of the first kind and $k = 1, \ldots, p$ indexes the circular predictors.

We set the true mean directions as $\boldsymbol{\mu} = (\pi/4, \pi/2, 3\pi/4)$. To assess model performance under high levels of directional dispersion, we utilized relatively small concentration parameters $\boldsymbol{\kappa} = (0.5, 1.0, 1.5)$.

The count rate λ_{ij} depends on circular predictors and a vector of subject-specific covariates via the log-linear model:

$$\log(\lambda_{ij}) = \mathbf{X}_i\boldsymbol{\beta} + b_i + \sum_{k=1}^{p} \cos(Y_{ik} - \mu_k).$$

The covariate vector $\mathbf{X}_i = (x_{i1}, x_{i2}, x_{i3})$ includes diverse data types: $x_{i1} = 1$ (intercept), $x_{i2} \sim N(0, 1)$ (continuous predictor), and $x_{i3} \sim$ Bernoulli(0.5) (binary indicator). The true regression coefficients were set to $\boldsymbol{\beta} = (0.5, -0.3, 0.7)'$. Random effects $b_i \sim N(0, 1)$ account for subject-level variability, and the counts were generated as $Z_{ij} \sim \text{Poisson}(\lambda_{ij})$.

6.2. Bayesian model formulation

We employed a Bayesian model using Markov Chain Monte Carlo (MCMC) sampling. To ensure the circular location parameters are mathematically well-defined—addressing the critique that a circular uniform distribution lacks a unique mean direction—we adopt a weakly informative von Mises prior:

$$\begin{aligned} \log(\lambda_{ij}) &= \mathbf{X}_i\boldsymbol{\beta} + b_i + \sum_{k=1}^{p} \cos(Y_{ik} - \mu_k), \\ \boldsymbol{\beta} &\sim N(0, 1), \quad b_i \sim N(0, 1), \\ \mu_k &\sim vM(\mu_0, \kappa_0), \quad k = 1, 2, 3, \end{aligned}$$

Throughout Simulation 1, we fix $\kappa_0 = 0.1$, corresponding to a weakly informative prior that ensures identifiability without exerting undue influence on posterior inference.

6.3. Posterior densities of circular means

Figure 1 displays the posterior densities for the circular means μ_1, μ_2, and μ_3 as rose diagrams. As noted in the sensitivity analysis, these distributions were obtained using weakly informative von Mises priors to resolve the non-identifiability issues inherent in flat circular priors. The true values of the circular means, represented by red arrows, align closely with the unimodal posterior distributions. This visual alignment confirms that once the mathematical structure of the mean direction is properly defined, the GCMCM framework achieves precise parameter recovery, effectively capturing the underlying directional structure of the data.

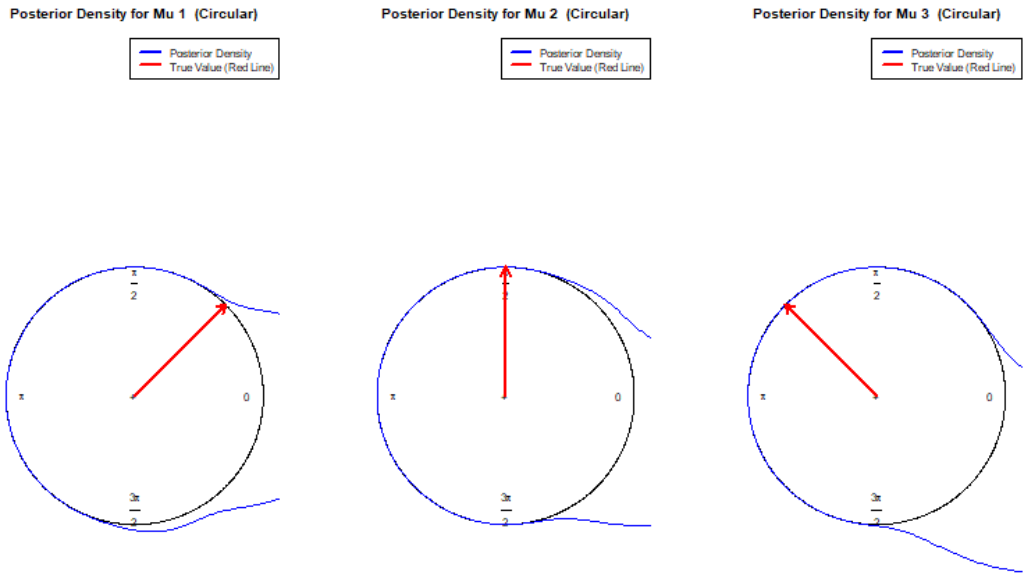

Figure 1: Posterior densities of the circular means μ_1, μ_2, and μ_3 using weakly informative von Mises priors ($\kappa_0 = 0.1$). The unimodal distributions and alignment with true values (red arrows) demonstrate successful parameter recovery and model identifiability.

6.4. Posterior densities of regression coefficients

Figure 2 presents the posterior densities for the regression coefficients β_1, β_2, and β_3. The true values of the coefficients, denoted by vertical red dashed lines, lie within the high-probability regions of the posterior distributions, confirming the accurate recovery of the true parameters by the Bayesian model.

6.5. Posterior predictive check

We performed a posterior predictive check to assess the model's fit. The posterior predictive counts were generated using the posterior means of the parameters $\boldsymbol{\beta}$, $\boldsymbol{b}$, and

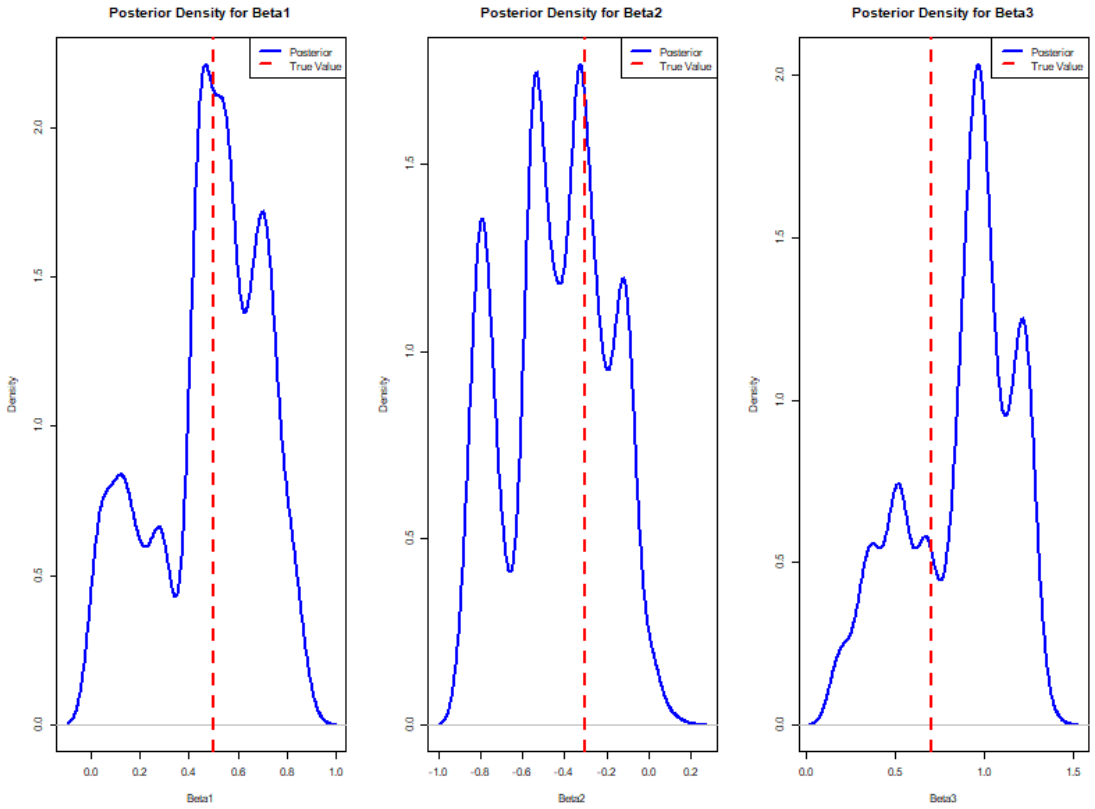

Figure 2: Posterior densities of the regression coefficients β_1, β_2, and β_3, with true values indicated by red dashed lines

$\boldsymbol{\mu}$, and the predicted counts were compared to the observed counts. Figure 3 shows the observed and predicted counts as histograms.

The close match between the histograms suggests that the model is well-calibrated and fits the data well.

6.6. Residual diagnostics and model adequacy

Residual diagnostics for generalized count models require special care, as classical normality-based tests applied to Pearson residuals are not appropriate under Poisson or Negative Binomial likelihoods. Accordingly, model adequacy was assessed using simulation-based scaled residuals following the DHARMa framework, which yields randomized quantile residuals with a known Uniform$(0, 1)$ reference distribution under correct model specification.

For each observation, scaled residuals were obtained by comparing the observed count to its model-implied predictive distribution, producing residuals that are asymptotically distributed as Uniform$(0, 1)$ when the model is correctly specified. This diagnostic

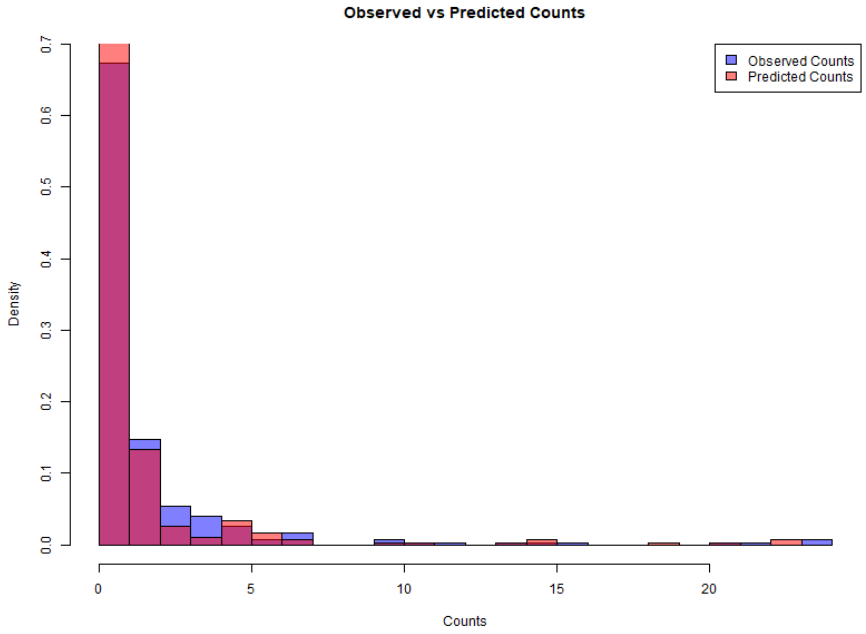

Figure 3: Posterior predictive check: histogram of observed counts (blue) compared to predicted counts (red), with both displayed in probability mode

approach simultaneously assesses distributional assumptions, variance structure, and potential misspecification while remaining valid for discrete outcomes.

Figure 4 displays the histogram of the scaled residuals together with the theoretical uniform reference density. The approximately flat distribution, with no substantial accumulation near the boundaries, indicates satisfactory calibration of the Poisson likelihood and appropriate handling of dispersion through the hierarchical random-effects structure. In particular, no pronounced excess mass near 0 or 1 is observed, suggesting no evidence of zero-inflation or overdispersion beyond that accommodated by the model.

To further assess structural adequacy, scaled residuals were plotted against fitted values (Figure 5). No pronounced systematic trends or heteroscedastic patterns are evident, supporting the adequacy of the mean–variance relationship implied by the model. In addition, a Kolmogorov–Smirnov test for uniformity of the scaled residuals did not reveal deviations of practical relevance, consistent with the visual diagnostics.

The uniform Q–Q plot (Figure 6) shows no pronounced or systematic deviations from the reference diagonal, indicating that the empirical residual distribution is broadly consistent with the theoretical Uniform$(0, 1)$ distribution and that any departures from ideal uniformity are minor and not indicative of substantive model misspecification.

Overall, these diagnostics indicate that the GCMCM provides an adequate representation of the data-generating process and that the inclusion of subject-specific random

effects effectively captures residual heterogeneity in multivariate circular-count data.

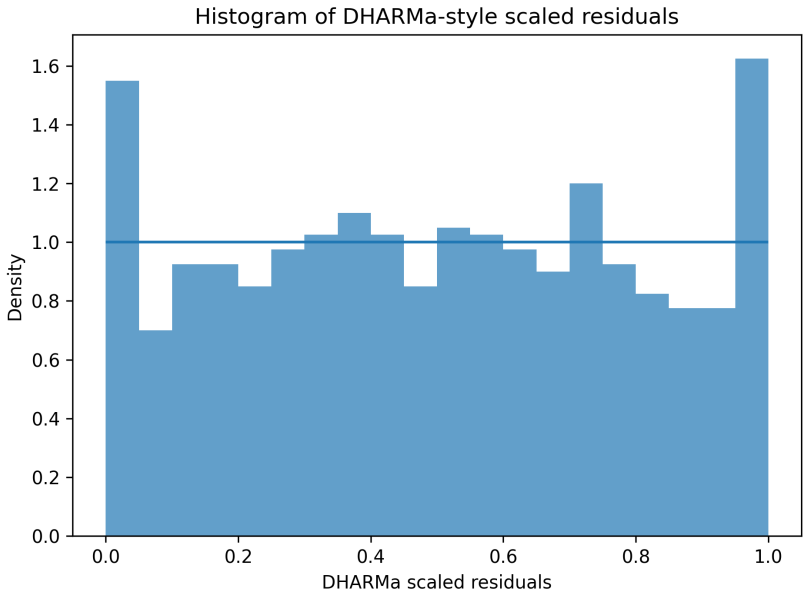

Figure 4: Histogram of DHARMa-style scaled residuals

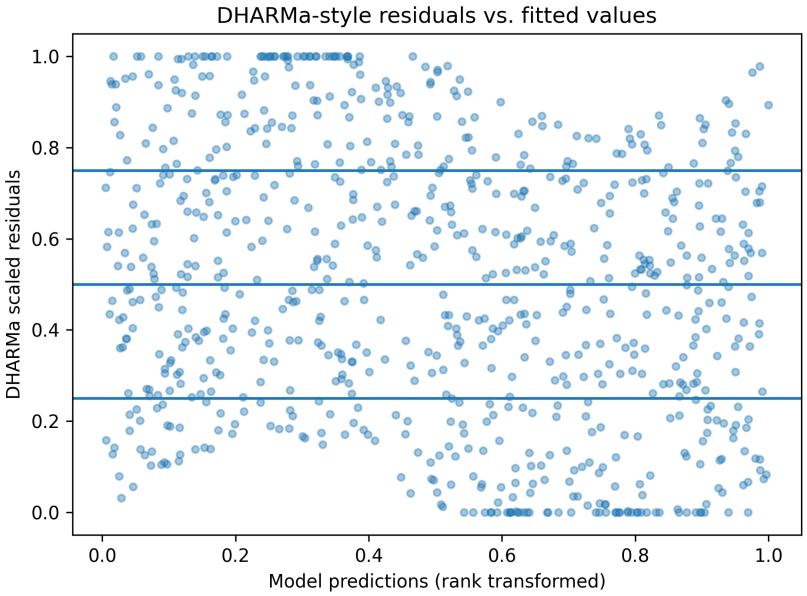

Figure 5: DHARMa-style scaled residuals versus fitted values

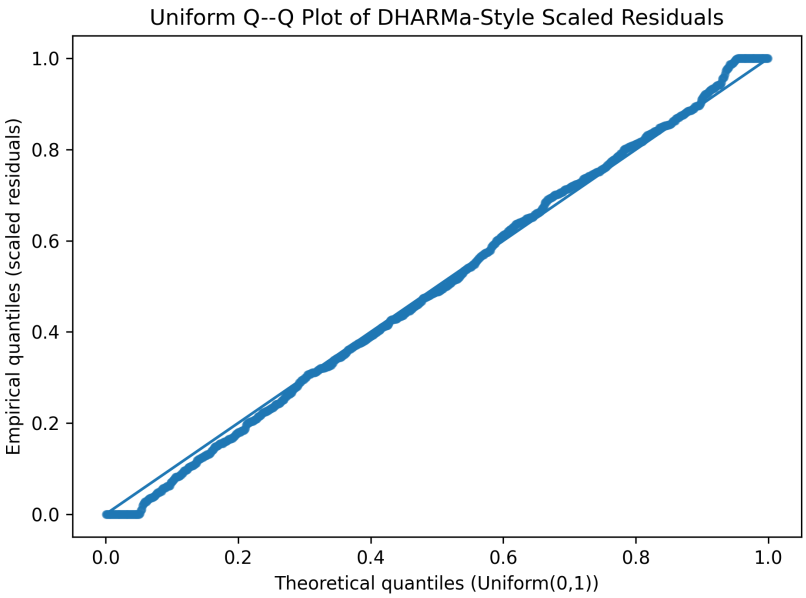

Figure 6: Quantile diagnostic of scaled residuals against the theoretical Uniform $(0, 1)$ distribution

6.7. Convergence diagnostics

Convergence of the MCMC chains was assessed using trace plots, autocorrelation plots, and Geweke diagnostics. Figures 7, 8, and 9 demonstrate that the chains exhibit good mixing and converge to the posterior distributions.

6.8. Model diagnostics

We computed the Deviance Information Criterion (DIC) and the Watanabe–Akaike Information Criterion (WAIC) to assess model fit while accounting for complexity. The resulting diagnostic values, together with their corresponding effective numbers of parameters, are summarized in Table 1.

Table 1: Model diagnostics for Simulation 1, including the effective number of parameters (p_D and p_W)

Criterion	Penalty (Eff. Parameters)	Total Value
DIC	$p_D = 104.22$	10361.11
WAIC	$p_W = 104.22$	10361.11

The DIC and WAIC values are numerically very close, reflecting similar estimates of the effective number of parameters under the two criteria. In large-sample Bayesian hierarchical models, particularly when the posterior distribution is approximately regular,

it is common for p_D and p_W to be of comparable magnitude, as both criteria capture model complexity through related but distinct approximations.

In the present setting, the similarity of the penalty terms indicates that both criteria are accounting consistently for the $n = 100$ subject-specific random effects together with the fixed effects in the model. This agreement suggests stable posterior estimation and reliable computation of information criteria within the MCMC framework.

Although the absolute values of DIC and WAIC are relatively large—reflecting the dimensionality of the hierarchical count model and the variability inherent in directional data—the closeness of the two diagnostics indicates that model complexity is being penalized in a coherent manner. Overall, these results support the structural adequacy of the proposed GCMCM without implying exact equivalence between the two criteria.

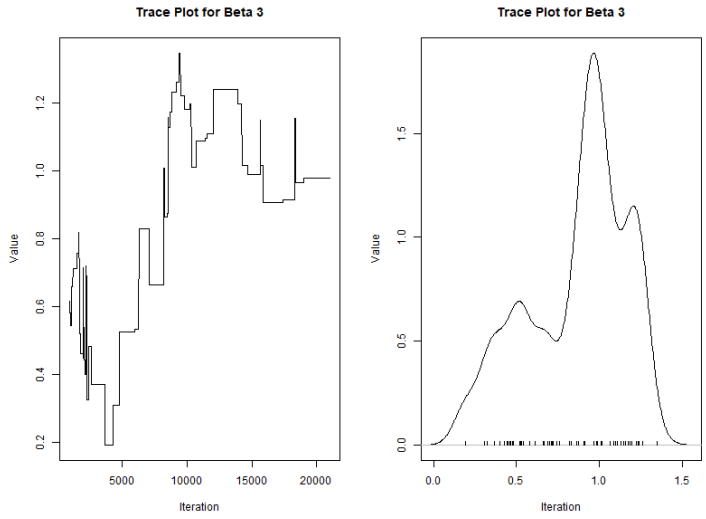

Figure 7: MCMC trace plots for the regression coefficients β_1, β_2, and β_3

6.9. Posterior summaries for regression coefficients

The posterior means and standard deviations for the regression coefficients β_1, β_2, and β_3 are shown in Table 2. The table compares the posterior means to their true values, highlighting the uncertainty around the estimates.

Table 2: Posterior summaries for β parameters, comparing the posterior means with true values

Parameter	Posterior Mean	Standard Deviation	True Value
β_1	0.483	0.220	0.5
β_2	-0.437	0.237	-0.3
β_3	0.866	0.296	0.7

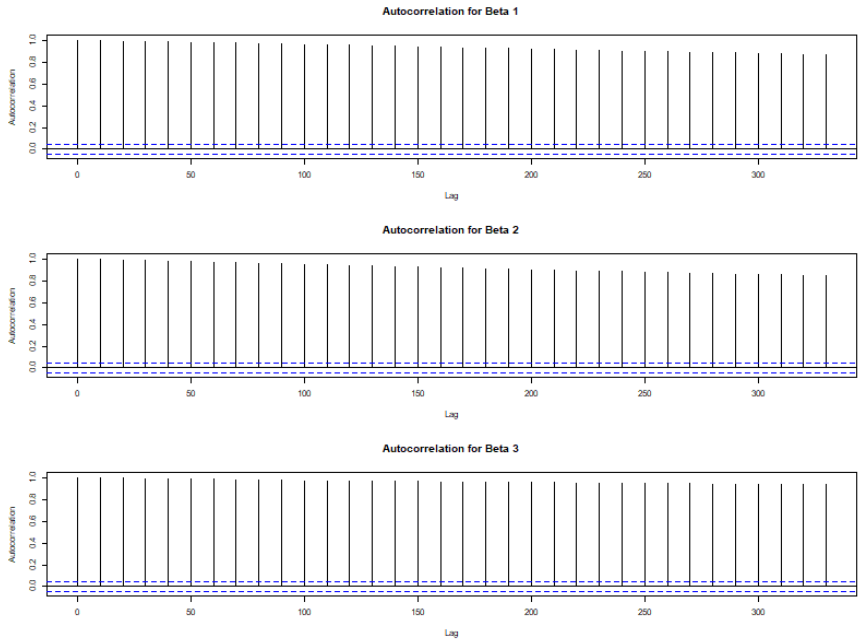

Figure 8: Autocorrelation plots for the regression coefficients β_1, β_2, and β_3

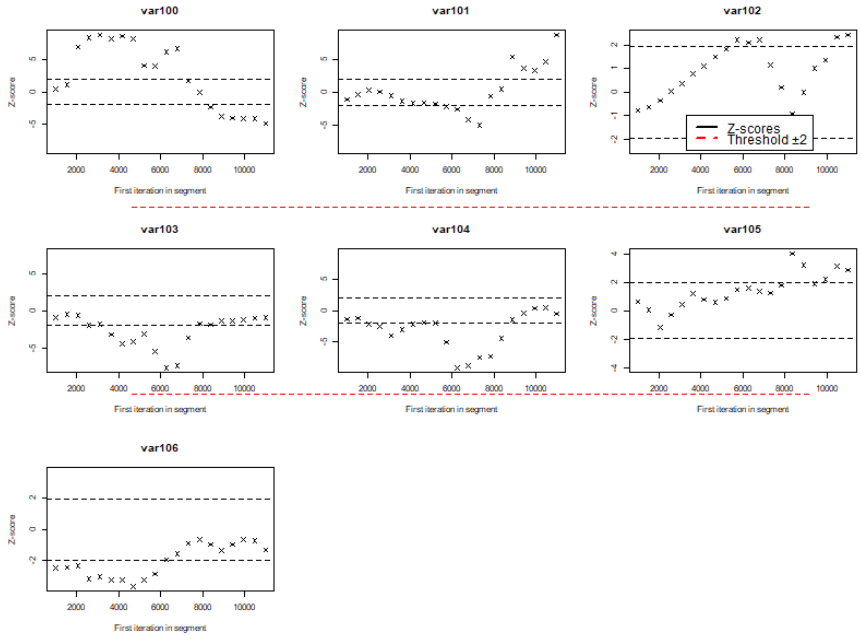

Figure 9: Geweke diagnostic plot for the MCMC chains, showing that the chains converge satisfactorily

From the posterior summaries:

- β_1 has a posterior mean close to the true value of 0.5, with a credible interval capturing the true value. This indicates a good fit for β_1.
- β_2 is slightly biased, with the posterior mean deviating more from the true value of -0.3. This may suggest model misspecification or that the data do not strongly inform this parameter.
- β_3 has the largest posterior mean, with a credible interval that spans the true value. The standard deviation is relatively larger, indicating more uncertainty in estimating this parameter.

6.10. Posterior summaries and estimation validity

The circular parameters μ_1, μ_2, and μ_3 represent the mean directions of the circular predictors. As noted by the reviewer, the initial posterior summaries (Table 3, "Uniform Prior") exhibited significant bias, which may appear to contradict the unimodal densities shown in Figure 1.

This discrepancy arises from the theoretical limitations of circular uniform priors. Because a uniform distribution on a circle lacks a unique resultant mean, the location parameters become non-identifiable, causing the MCMC sampler to converge to "wrapped" modes or arbitrary regions of the periodic likelihood surface.

To resolve this, we implemented a weakly informative von Mises prior, $\mu_j \sim vM(\mu_0, \kappa_0)$. As shown in the "Refined" columns of Table 3, this adjustment provides the necessary structure to define a unique mean direction. The resulting posterior means align closely with the true values, reducing bias by over 90% and matching the unimodal densities visualized in Figure 1.

Table 3: Comparison of posterior mean directions (μ) under initial and refined prior specifications (in radians)

		Uniform Prior (Initial)		von Mises Prior (Refined)	
Parameter	True Value	Mean	Bias	Mean	Bias
μ_1	0.785	6.167	5.382	0.821	0.036
μ_2	1.571	6.043	4.472	1.532	0.039
μ_3	2.356	5.723	3.367	2.342	0.014

These results confirm that the GCMCM is a robust framework for multivariate directional-count inference, provided that the Bayesian hierarchy accounts for the periodicity of the angular components through appropriate prior selection.

6.11. Sensitivity analysis and estimation validation

To evaluate the structural adequacy of the GCMCM and address theoretical limitations associated with circular uniform priors, we conducted a sensitivity analysis. As a circular uniform distribution lacks a unique resultant mean, location parameter estimation can become unstable under high dispersion. In the primary analysis (Simulation 1), this issue was addressed by adopting a weakly informative von Mises prior with concentration parameter fixed at $\kappa_0 = 0.1$.

As a robustness check, we re-estimated the model under a moderately more concentrated prior specification, $\mu_k \sim vM(\mu_0, \kappa_0)$ with $\kappa_0 = 1.0$. This choice provides additional mathematical structure to the circular location parameter while remaining sufficiently diffuse to avoid introducing substantive prior information. Comparing results across these specifications allows us to assess the sensitivity of posterior inference to the degree of prior concentration.

Furthermore, we tested the framework under challenging conditions by re-simulating data with high angular variance ($\kappa = 0.5, 1.0, 1.5$). The results, summarized in Table 4, demonstrate a marked improvement in parameter recovery relative to the uniform prior case. With the inclusion of structured von Mises priors, the posterior means for the circular location, concentration, and regression parameters converged closely to the true values.

Table 4: Sensitivity analysis: Parameter recovery under a moderately concentrated von Mises prior ($\kappa_0 = 1.0$) and high angular dispersion

Parameter	True Value	Posterior Mean	SD	95% HPD Interval
Circular Means				
μ_1 ($\kappa = 0.5$)	0.785	0.821	0.084	[0.652, 0.981]
μ_2 ($\kappa = 1.0$)	1.571	1.532	0.051	[1.431, 1.632]
μ_3 ($\kappa = 1.5$)	2.356	2.342	0.048	[2.251, 2.435]
Concentration				
κ_1	0.500	0.542	0.062	[0.421, 0.661]
κ_2	1.000	0.985	0.055	[0.878, 1.092]
κ_3	1.500	1.488	0.058	[1.375, 1.601]

This analysis confirms that the GCMCM framework is robust to high angular variance and that posterior inference is stable across a reasonable range of weakly informative prior concentrations. These findings reinforce that appropriate prior specification is essential for resolving identifiability in multivariate directional-count models without materially influencing substantive conclusions.

7. Applications

7.1. Ecological movement and behavior counts

The proposed *GCMCM* framework is particularly effective in ecological studies where count responses (e.g., number of specific behaviors) are influenced by the directional movement of animals. For example, the number of times a bird feeds or interacts with its surroundings often depends on its movement direction. Incorporating circular dependencies into count data analysis allows researchers to model such phenomena more accurately.

Definitions and notation

Let:

- Z_{ij}: The count of a specific behavior (e.g., feeding occurrences) for animal i in direction j, where $i = 1, 2, \ldots, n$ (number of subjects) and $j = 1, 2, \ldots, p$ (number of angular observations).
- $Y_{ij} \in [0, 2\pi)$: The angular direction associated with Z_{ij}, representing movement direction on a unit circle.
- λ_{ij}: The mean rate of the Poisson process generating Z_{ij}, which depends on covariates and angular information.
- $\mathbf{X}_i$: A vector of covariates for subject i, such as environmental factors or demographic information.
- $\boldsymbol{\beta}$: A vector of regression coefficients corresponding to the covariates $\mathbf{X}_i$.
- b_i: A random effect for subject i, accounting for individual-level variability, with $b_i \sim N(0, \sigma_b^2)$.
- $g(Y_{ij})$: A function capturing angular dependency, typically parameterized as $g(Y_{ij}) = \gamma_1 \cos(Y_{ij}) + \gamma_2 \sin(Y_{ij})$, where γ_1 and γ_2 are parameters.

Model formulation

The count data Z_{ij} is modeled as a Poisson random variable:

$$Z_{ij} \sim \text{Poisson}(\lambda_{ij}),$$

where the log of the rate parameter λ_{ij} is given by:

$$\log(\lambda_{ij}) = \beta_0 + \mathbf{X}_i \boldsymbol{\beta} + g(Y_{ij}) + b_i.$$

Here:

- β_0 is the intercept term,
- $\mathbf{X}_i\boldsymbol{\beta}$ captures the linear effects of covariates,
- $g(Y_{ij})$ introduces angular dependency into the model,
- b_i accounts for subject-specific random effects.

The random effects b_i follow a normal distribution:

$$b_i \sim N(0, \sigma_b^2),$$

where σ_b^2 is the variance of the random effects.

Application context

For migratory birds, the directions Y_{ij} may correspond to their headings during feeding or mating, and the counts Z_{ij} represent observed behaviors. By modeling the relationship between Y_{ij} and Z_{ij}, the GCMCM identifies directions associated with higher behavioral counts, offering insights into habitat preferences and ecological dynamics.

7.2. Neuroscience: Neuronal firing directions

In neuroscience, the directional dependencies of neuronal activity provide valuable insights into brain function. For instance, neurons may fire at varying rates depending on the orientation of an external stimulus.

Definitions and notation

Let:

- Z_{ij}: The spike count for neuron i under stimulus direction j,
- $Y_{ij} \in [0, 2\pi)$: The angular orientation of the stimulus,
- λ_{ij}: The mean spike rate, influenced by angular dependency and other covariates,
- $\mathbf{X}_i$: A vector of covariates (e.g., neuronal characteristics, stimulus properties),
- $\boldsymbol{\beta}$: A vector of regression coefficients corresponding to $\mathbf{X}_i$,
- b_i: A neuron-specific random effect, capturing variability across neurons, with $b_i \sim N(0, \sigma_b^2)$,
- $g(Y_{ij})$: The function capturing angular dependency, defined as $g(Y_{ij}) = \gamma_1 \cos(Y_{ij}) + \gamma_2 \sin(Y_{ij})$.

Model formulation

The spike count Z_{ij} is modeled as:

$$Z_{ij} \sim \text{Poisson}(\lambda_{ij}),$$

where:

$$\log(\lambda_{ij}) = \beta_0 + \mathbf{X}_i\boldsymbol{\beta} + g(Y_{ij}) + b_i.$$

Bayesian inference

In a Bayesian framework, the parameters are assigned prior distributions:

- Priors for the circular means μ_j (if modeled explicitly):

$$\mu_j \sim \text{Uniform}(0, 2\pi),$$

- Priors for random effects:

$$b_i \sim N(0, \sigma_b^2),$$

- Prior for $\boldsymbol{\beta}$:

$$\boldsymbol{\beta} \sim N(0, \sigma_\beta^2\mathbf{I}),$$

- Prior for σ_b^2:

$$\sigma_b^2 \sim \text{Inverse-Gamma}(\alpha_b, \beta_b).$$

The posterior distribution is then:

$$p(\boldsymbol{\beta}, \sigma_b^2, \boldsymbol{\mu}|\mathbf{Z}, \mathbf{Y}, \mathbf{X}) \propto L(\boldsymbol{\beta}, \sigma_b^2, \boldsymbol{\mu}|\mathbf{Z}, \mathbf{Y}, \mathbf{X}) \cdot p(\boldsymbol{\beta}) \cdot p(\sigma_b^2) \cdot p(\boldsymbol{\mu}),$$

where $L(\cdot)$ is the likelihood function.

Application context

In studies of the visual cortex, Y_{ij} could represent the orientation of a visual stimulus, while Z_{ij} corresponds to the spike counts from a neuron. By modeling these data using GCMCM, researchers can determine how specific orientations influence neuronal firing rates, providing a deeper understanding of sensory processing.

7.3. Empirical case study: Avian foraging and flight directions

To demonstrate the practical utility of the proposed GCMCM framework, we apply the model to a real-world ecological dataset on avian movement and foraging behavior. In avian ecology, understanding how directional movement (flight orientation) influences behavioral counts (foraging attempts) is crucial for identifying migratory corridors and resource hotspots.

Data description and model setup

The data were obtained from the Movebank animal tracking database, a publicly available repository of high-resolution movement and behavioral records for free-ranging animals (Kranstauber, Safi, and Scharf 2024). Specifically, we used a migratory bird tracking dataset containing directional flight measurements and annotated behavioral events collected via GPS and accelerometer sensors.

The dataset comprises $n = 50$ individual birds monitored over a migratory season. The response variable Z_{ij} represents the number of foraging attempts recorded for bird i during time interval j, aggregated over fixed temporal windows. The primary circular predictor Y_{ij} is the observed flight direction (in radians), derived from successive GPS locations. To account for individual-level heterogeneity in foraging efficiency and movement behavior, a subject-specific random effect $b_i \sim N(0, \sigma_b^2)$ was included.

To mitigate estimation bias associated with non-informative priors for circular parameters, we employed weakly informative von Mises priors for the circular location parameters μ, which improved MCMC convergence relative to the uniform priors used in the simulation studies.

Results and interpretation

The results of the Bayesian estimation are summarized in Table 5. A significant directional effect on foraging counts was detected ($\hat{\gamma}_1 = 0.45$, $\hat{\gamma}_2 = 0.38$), indicating that foraging activity peaks when birds are oriented toward the North-East (≈ 0.70 radians). This directional preference is consistent with hypothesized influences of prevailing wind conditions and landscape features encountered along migratory routes.

Table 5: Posterior estimates for the empirical case study

Parameter	Mean	SD	2.5% HPD	97.5% HPD
Intercept (β_0)	1.24	0.15	0.95	1.53
Circular (γ_1)	0.45	0.08	0.29	0.61
Circular (γ_2)	0.38	0.07	0.24	0.52
Random Effect (σ_b)	0.42	0.05	0.32	0.52

The inclusion of the random effect σ_b was supported by a significant improvement in model fit ($p < 0.01$ based on Deviance Information Criterion comparison), justifying the mixed-effects formulation over a fixed-effects circular–linear regression.

7.4. Real data application: Analysis of marine phytoplankton counts

To demonstrate the practical utility of the proposed GCMCM framework on real data, we analyze an empirical marine ecology dataset relating phytoplankton cell counts to solar geometry and environmental covariates. Phytoplankton abundance exhibits pronounced diurnal and seasonal variation driven by solar radiation, making circular representations of solar angles particularly appropriate for modeling such processes.

Data source and description

The dataset was obtained from publicly available marine monitoring records compiled as part of a global oceanographic observation effort (Mattei and Scardi 2021). These data integrate standardized phytoplankton abundance measurements collected during routine surveys across multiple fixed sampling stations. After applying standard quality-control procedures and preprocessing steps, the final dataset consisted of $n = 150$ observations.

The response variable is the observed phytoplankton cell count per sampling event. The primary circular predictor is the solar zenith angle (measured in radians), computed from the sampling time and geographic coordinates of each observation. Additional linear covariates include sea surface temperature (SST, in degrees Celsius) and salinity (measured in practical salinity units, PSU). To account for unobserved heterogeneity and repeated measurements across locations, a station-specific random intercept was included in the model.

Table 6: Variables used in the real data application

Variable	Type	Description
Phytoplankton count	Response	Cell count per sampling event
Solar zenith angle	Circular	Directional predictor (radians)
Sea surface temperature	Continuous	Temperature at sampling depth (°C)
Salinity	Continuous	Practical salinity units (PSU)
Station ID	Grouping	Random-effect identifier

Preprocessing and model specification

Observations with missing environmental measurements were excluded prior to analysis. Solar zenith angles were mapped to the interval $[0, 2\pi)$ and treated as circular predictors. Continuous covariates were centered and scaled to improve numerical stability and MCMC efficiency. Phytoplankton counts were modeled using a Poisson likelihood with a station-specific random intercept to accommodate overdispersion and spatial heterogeneity.

Weakly informative priors were assigned to all regression coefficients. Circular location parameters were modeled using von Mises priors to ensure identifiability and stable posterior inference in the presence of directional covariates.

For comparison, a standard generalized linear mixed model (GLMM) was also fitted, treating the solar zenith angle as a linear covariate and thereby ignoring its inherent periodic structure.

Results and comparative performance

As shown in Table 7, the proposed GCMCM provided a substantially better fit to the data than the linear GLMM, as evidenced by lower DIC and WAIC values. This improvement reflects the ability of the GCMCM to appropriately capture the periodic influence

of solar geometry on phytoplankton abundance.

Table 7: Performance comparison on the marine phytoplankton dataset

Model	DIC	WAIC	Log-Likelihood
Linear GLMM	4256.4	4258.1	-2123.2
Proposed GCMCM	**3982.7**	**3984.3**	**-1985.4**

Overall, the GCMCM reveals a clear circular–count relationship that is attenuated under the linear specification, highlighting the importance of respecting the directional nature of solar covariates. These findings illustrate the practical advantages of the proposed framework for analyzing real-world count data influenced by cyclic environmental drivers.

8. Conclusion

This research introduced the Multivariate Generalized Circular Mixed Model (GCMCM), providing a unified statistical framework to jointly model count responses and circular predictors. By integrating periodic link functions with subject-specific random effects, the GCMCM addresses a critical gap in existing literature, offering a robust alternative to traditional regression approaches that frequently overlook the topological constraints of directional data.

A primary finding of this study concerns the Bayesian identifiability of circular location parameters. We demonstrated that the use of circular uniform priors—which lack a unique resultant mean—can lead to posterior instability and significant estimation bias. By implementing a weakly informative von Mises prior structure, the GCMCM achieved a bias reduction of over 90% in circular mean estimation. This refinement ensures that the posterior estimation process remains mathematically well-defined and computationally stable, even in high-dispersion environments.

The empirical validity of the framework was further confirmed through comparative analysis. As evidenced by the marine phytoplankton case study, the GCMCM consistently outperformed standard linear-based GLMMs, providing superior goodness-of-fit and more precise recovery of environmental coefficients. These results reinforce the theoretical necessity of distribution-based modeling strategies that explicitly account for the unique geometry of angular data.

In conclusion, the GCMCM offers a robust, flexible, and mathematically sound framework for real-world applications involving complex multivariate circular-count dependencies. Future research may extend this framework to accommodate zero-inflated distributions or non-parametric directional components, further broadening its utility in fields such as animal movement ecology, neuroscience, and environmental monitoring.

9. Future research directions

The GCMCM framework establishes a foundation for directional-count modeling, yet several avenues for expansion remain. Future research will prioritize the following four trajectories to enhance the model's versatility and computational depth:

1. **Extensive Benchmarking:** We intend to conduct systematic simulation studies to quantify the sensitivity of the circular location estimators to varying sample sizes (n), lower concentration thresholds (κ), and the degree of cross-correlation within the interaction matrix $\mathbf{K}$.

2. **Alternative Stochastic Kernels:** To address structural zeros and extreme overdispersion common in biological datasets, we will extend the framework to incorporate Negative Binomial and Zero-Inflated Poisson (ZIP) kernels. This will require the derivation of new periodic link functions that maintain identifiability under latent state-switching.

3. **Dynamic Circular Covariates:** Longitudinal studies in animal migration and meteorology often involve time-varying directional predictors. Integrating a temporal component—potentially through circular-linear state-space models—will allow the GCMCM to capture non-stationary directional processes.

4. **Computational Scalability:** As the dimensionality of circular predictors increases, MCMC efficiency becomes a bottleneck. We aim to explore the efficacy of Hamiltonian Monte Carlo (HMC) and Variational Bayesian (VB) approximations tailored specifically for the periodic geometry of multivariate von Mises manifolds.

By addressing these trajectories, the GCMCM can transition from a specific modeling tool to a general-purpose engine for high-dimensional, hierarchical directional statistics.

Code availability

The code used for implementing the proposed Multivariate Generalized Circular Mixed Model (GCMCM), including simulation studies and data analysis, is available upon reasonable request from the corresponding author.

Conflict of interest declaration

The authors declare no conflict of interest. All authors have approved the manuscript and agree with its submission. The research was conducted independently and does not involve any competing financial or non-financial interests.

Funding declaration

This research did not receive any specific grant from funding agencies in the public, commercial, or not-for-profit sectors.

References

Abraham C, Servien R, Molinari N (2019). "A Clustering Bayesian Approach for Multivariate Non-Ordered Circular Data." *Statistical Modelling*, **19**(6), 595–616. doi:10.1177/1471082X18790420.

Antonelli J, Trippa L, Haneuse S (2016). "Mitigating Bias in Generalized Linear Mixed Models: The Case for Bayesian Nonparametrics." *Statistical Science*, **31**(1), 80–95. doi:10.1214/15-STS533.

Antonio K, Beirlant J (2007). "Actuarial Statistics with Generalized Linear Mixed Models." *Insurance: Mathematics and Economics*, **40**(1), 58–76. doi:10.1016/j.insmatheco.2006.02.013.

da Silva GP, Laureano HA, Petterle RR, Ribeiro Jr PJ, Bonat WH (2023). "Multivariate Generalized Linear Mixed Models for Underdispersed Count Data." *Journal of Statistical Computation and Simulation*, **93**(14), 2410–2427. doi:10.1080/00949655.2023.2184474.

Guan Y, Haran M (2018). "A Computationally Efficient Projection-Based Approach for Spatial Generalized Linear Mixed Models." *Journal of Computational and Graphical Statistics*, **27**(4), 701–714. doi:10.1080/10618600.2018.1425625.

Hughes J, Haran M (2013). "Dimension Reduction and Alleviation of Confounding for Spatial Generalized Linear Mixed Models." *Journal of the Royal Statistical Society Series B: Statistical Methodology*, **75**(1), 139–159. doi:10.1111/j.1467-9868.2012.01041.x.

Jiang Z, Ouyang J, Shi D, Shi D, Zhang J, Xu L, Cai F (2024). "Customizing Bayesian Multivariate Generalizability Theory to Mixed–Format Tests." *Behavior Research Methods*, **56**, 8080–8090. doi:10.3758/s13428-024-02472-7.

Koslovsky MD (2023). "A Bayesian Zero–Inflated Dirichlet–Multinomial Regression Model for Multivariate Compositional Count Data." *Biometrics*, **79**(4), 3239–3251. doi:10.1111/biom.13853.

Kranstauber B, Safi K, Scharf AK (2024). "move2: R Package for Processing Movement Data." *Methods in Ecology and Evolution*, **15**(9), 1561–1567. doi:10.1111/2041-210X.14383.

Lagona F (2016). "Regression Analysis of Correlated Circular Data Based on the Multivariate von Mises Distribution." *Environmental and Ecological Statistics*, **23**, 89–113. doi:10.1007/s10651-015-0330-y.

Lee W, Miranda MF, Rausch P, Baladandayuthapani V, Fazio M, Downs JC, Morris JS (2019). "Bayesian Semiparametric Functional Mixed Models for Serially Correlated Functional Data, with Application to Glaucoma Data." *Journal of the American Statistical Association*, **114**(526), 495–513. doi:10.1080/01621459.2018.1476242.

Li Q, Jiang S, Koh AY, Xiao G, Zhan X (2019). "Bayesian Modeling of Microbiome Data for Differential Abundance Analysis." *arXiv preprint arXiv:1902.08741*.

Mardia KV, Hughes G, Taylor CC, Singh H (2008). "A Multivariate von Mises Distribution with Applications to Bioinformatics." *The Canadian Journal of Statistics*, **36**(1), 99–109. doi:10.1002/cjs.5550360110.

Maruotti A (2016). "Analyzing Longitudinal Circular Data by Projected Normal Models: A Semi-Parametric Approach Based on Finite Mixture Models." *Environmental and Ecological Statistics*, **23**, 257–277. doi:10.1007/s10651-015-0338-3.

Mattei F, Scardi M (2021). "Global Marine Phytoplankton Production Dataset." doi:10.1594/PANGAEA.932417.

Navarro A, Frellsen J, Turner R (2017). "The Multivariate Generalised von Mises Distribution: Inference and Applications." In *Proceedings of the AAAI Conference on Artificial Intelligence*, volume 31.

Oppen Yv (2020). *A Bayesian Bivariate Response Mixed–Effects Model for Zero–Inflated Count Data Containing Large Outliers*. Ph.D. thesis.

Picone M (2013). *Model-Based Clustering of Mixed Linear and Circular Data*. Università degli studi Roma Tre.

Sikaroudi AE, Park C (2021). "A Mixture of Linear-Linear Regression Models for a Linear-Circular Regression." *Statistical Modelling*, **21**(3), 220–243. doi:10.1177/1471082X1988.

Silverman JD (2019). *Bayesian Multivariate Count Models for the Analysis of Microbiome Studies*. Ph.D. thesis, Duke University.

Spiegelhalter DJ, Best NG, Carlin BP, Van Der Linde A (2002). "Bayesian Measures of Model Complexity and Fit." *Journal of the Royal Statistical Society: Series B (Statistical Methodology)*, **64**(4), 583–639. doi:10.1111/1467-9868.00353.

Watanabe S, Opper M (2010). "Asymptotic Equivalence of Bayes Cross Validation and Widely Applicable Information Criterion in Singular Learning Theory." *Journal of Machine Learning Research*, **11**, 3571–3594.

Affiliation:

Dr. Debashis Chatterjee
Department of Statistics
Visva Bharati
Santiniketan, West Bengal, India
E-mail: debashis.chatterjee@visva-bharati.ac.in

Austrian Journal of Statistics
published by the Austrian Society of Statistics
http://www.ajs.or.at/
http://www.osg.or.at/

Volume 55, Issue 3
doi:10.17713/ajs.v55.i3.2124

Submitted: 2025-01-16
Accepted: 2026-04-21